Interaction between a Pulsating Flow and a Perforated Membrane

Raphael Lardat* — **Romuald Carpentier*** — **Bruno Koobus****
Eric Schall*** — **Alain Dervieux*** — **Charbel Farhat******
Jean-François Guery***** — **Patrick Della Piéta*******

** INRIA, 2003 Route des Lucioles, F-06902 Sophia-Antipolis Cedex, Raphael.Lardat@Inria.fr, Alain.Dervieux@Inria.fr*
*** Université de Montpellier II, Place Eugène Bataillon, Département de Mathématiques, CC 051, F-34095 Montpellier Cedex 5 and INRIA, koobus@math.univ-montp2.fr*
**** Université de Pau, IUT Génie Thermique et Energétique, 1, Avenue de l'Université, F-64000 PAU, Eric.Schall@univ-pau.fr*
***** University of Colorado at Boulder, Campus Box 429, Dept. of Aerospace Eng. Sciences, Boulder, COLORADO 80309-0429, U.S.A, charbel@boulder.colorado.edu*
****** Société Nationale des Poudres et Explosifs, B.P. 2, F-91760 Vert le Petit, JF.Guery@propulsion.snpe.com, P.DellaPieta@propulsion.snpe.com*

ABSTRACT. *A fully ALE 3D approach involving a Navier-Stokes solver is applied to the study of the interaction of a pulsating flow in a tube with a perforated diaphragm. We concentrate on an inviscid flow and the structure is modelled through shell elements. The effect on the first mode of the structure is examined with the study of the influence of the pulsation amplitude and of the pulsation frequency.*

RÉSUMÉ. *On considère l'interaction entre un écoulement pulsé et une membrane perforée. Cette étude utilise une approche ALE 3D comprenant un noyau Navier-Stokes. L'écoulement est de type non visqueux et la structure est modélisée par des éléments coques. L'effet du premier mode structure sur la réponse aéroélastique est plus particulièrement examiné en étudiant l'influence de l'amplitude de la pulsation ainsi que l'influence de la fréquence de pulsation.*

KEYWORDS: *fluid/structure interaction, pulsating flow, diaphragm, Euler equations*

MOTS-CLÉS : *interaction fluide/structure, écoulement pulsé, membrane, équations d'Euler*

Revue européenne des éléments finis. Volume 9 – n° 6-7/2000, pages 805 à 817

1. Introduction

Increasing scales of artifacts leads frequently to various unexpected difficulties. It is well known that bigger aircrafts, for example, have to manage with much wider structural deformations, which are consequences of the coupling between structural and aerodynamical effects. In the ARIANE5 programme, the two lateral boosters are about one order of magnitude heavier than those of ARIANE4, and this motivates several prospective studies started in order to ensure that performances and safety will not be affected (or how it will be affected) by new coupling phenomena.

Large Solid Rocket Motors (SRM) are generally not made of one piece, but involve segments often separated by thermal inhibitors. During the combustion of the solid propellant, the inhibitors become obstacles to the flow which may induce vortices. Even if this mechanism is not the only one leading to vortex-shedding, the passing of vortices through the outlet nozzle induce a fluctuation of internal pressure, and therefore of thrust, which leads to a rather complex aero-acoustic coupling showing a variety of quasi-periodic solution [CAR 99] and [CAR 98]. This has been analyzed in the ASSM research and technology french programme for which physical and numerical model have been developed for predicting thrust oscillation levels in SRM [LEB 99]. Some attempts have been done in 3D [MON 99] but remain very expensive.

It is clear that the final target problem for a complete study of membrane-flow interaction should involve the calculation of the complete geometry of the SRM, in order to compute in a coupled manner both aero-acoustics and structure. This is a very ambitious programme in terms of computer efforts, that has to be prepared by less heavy preliminary studies. We propose in this paper the academic study of a prescribed pulsating flow interacting with a membrane.

The modelization and software involves a finite-element dynamical shell model for the structure, and a finite-element finite-volume upwind Euler model for the flow. Coupling between both models is built through a full ALE formulation for the fluid, and proper transmission of efforts through a non-conforming discrete interface, see [FAR 98]. Special care has been paid to space-time integration, (see [FAR 95]).

The purpose of the present paper is to give a first glance of a few mechanical issues concerning the fluid-structure interaction, and to analyse the numerical questions related to their accurate prediction by the proposed methods.

Already many fluid-structure interaction systems have been studied and calculated with various methods. The present SRM problem does not seem having been studied in the litterature. Restricting to compressible flows, we would say that most contributions have been focusing on aerodynamic flutter at different regimes (see for example [FAR 95]). Other related contexts consider only acoustics-structure coupling, without flow modelling. The original features of the mechanical system we consider is the rather low Mach recirculating flow, involving density variations, and also acoustics.

The plan of the paper is as follows:

- about numerical model,
- recirculating flow,
- structural modes,
- static effects,
- effects of pulsations.

2. About numerical model

2.1. *Generic properties*

The numerical tool is exactly the same as the one used in the brothers papers in this issue [SCH 99] and [LAR 00]. In short, it relies on an unsteady three-field model consisting of a structural model (a shell), a fluid model (compressible Reynolds-Averaged Navier-Stokes), a pseudo-elasticity model for the dynamical fluid mesh. It is useful for the sequel to give a few equations describing the coupled model:

$$\begin{aligned} \frac{\partial}{\partial t}(V(x,t)w(t)) + F^c(w(t),x,\dot{x}) &= R(w(t),x) \\ M\frac{\partial^2 q}{\partial t^2} + f^{int}(q) &= f^{ext}(w(t),x) \\ \tilde{M}\frac{\partial^2 x}{\partial t^2} + \tilde{D}\frac{\partial x}{\partial t} + \tilde{K}x &= K_c q \end{aligned} \qquad [1]$$

where t designates time, x the position of a moving fluid grid point, w is the fluid state vector, V results from the finite element/volume discretization of the fluid equations, F^c is the vector of convective ALE fluxes, R is the vector of diffusive fluxes, q is the structural displacement vector, f^{int} denotes the vector of internal forces in the structure, f^{ext} the vector of external forces, M is the finite element mass matrix of the structure, $\tilde{M}$, $\tilde{D}$ and $\tilde{K}$ are fictitious mass, damping and stiffness matrices associated with the moving fluid grid and K_c is a transfer matrix that describes the action of the motion of the structural side of the fluid/structure interface on the fluid dynamic mesh.

An implicit time advanced finite-element scheme is used for the structural model and an implicit time advanced, time-staggered with respect to structure, vertex-centered upwind finite volume scheme is used for the fluid part.

Numerical options address second order accuracy both in space and time [FAR 95].

2.2. *Specific options*

In the sequel a subsonic flow in a duct is considered. The shock capturing facilities in the fluid model are inhibited ("no limiter"). Moreover, in order to obtain a low

level of numerical dissipation, a scalar coefficient γ is used to weight the numerical viscosity introduced by the Roe approximate Riemann solver (L for left, R for right):

$$\begin{aligned} Flux(W_L, W_R, n) &= 0.5\,(Flux(W_L, W_L, n) + Flux(W_R, W_R, n)) \\ &- 0.5\,\gamma\,|J|(W_L - W_R) \end{aligned} \quad [2]$$

in which n is the normal vector to cell boundary and J the Jacobian of fluxes times the normal n. Usual option is $\gamma = 1$ for standard Roe solver, and for lower values of numerical viscosity, smaller values of γ will be preferred.

Considering the accuracy issue, and since the global flow is of a medium-small Mach number, we found it useful to compare between the above option and the use of the Turkel preconditionner combined with the Roe splitting. It has been noted in many papers [GUI 98] that this preconditioner is very useful for accuracy. We however observed only a small improvement in accuracy (at the price of a slightly degraded time stability) when using the Turkel preconditioner; the explanation is that Mach number is not low enough. Therefore, the option in this paper is not to use the preconditioner.

The choice of in/out boundary conditions was *a priori* a sensitive one. Indeed, the geometry is assumed infinitely long, and a truncation is applied on the discrete level. This is then similar to external flows where farfield conditions should account for both a large distance, and non-reflexive properties. At the same time, it is important that the inflow information (pulsation) be introduced in a sufficiently strong mode in the computational domain. We have compared several issues and fixed our choice on a Steger-Warming flux splitting:

$$Flux(W_b, W_\infty, n) = J(W_b)^+ W_b + J(W_b)^+ W_\infty \quad [3]$$

where W_b stands for the boundary degree of freedom and W_∞ the in/out farfield imposed state vector.

3. Recirculating flow

This section aims at giving a few information about the flow topology before its coupling with the structure.

3.1. *Definition of the geometry*

The geometry is made of a circular cylinder, which contains a diaphragm with a circular hole at its mid-length. An idea of the fluid mesh is given in Figs. 1 and 2.

3.2. *Numerical flow behavior*

The flow is much accelerated by the diaphragm, by a factor 10; a jet is created there and keeps a rather constant section until outlet. The recirculating zones occurring

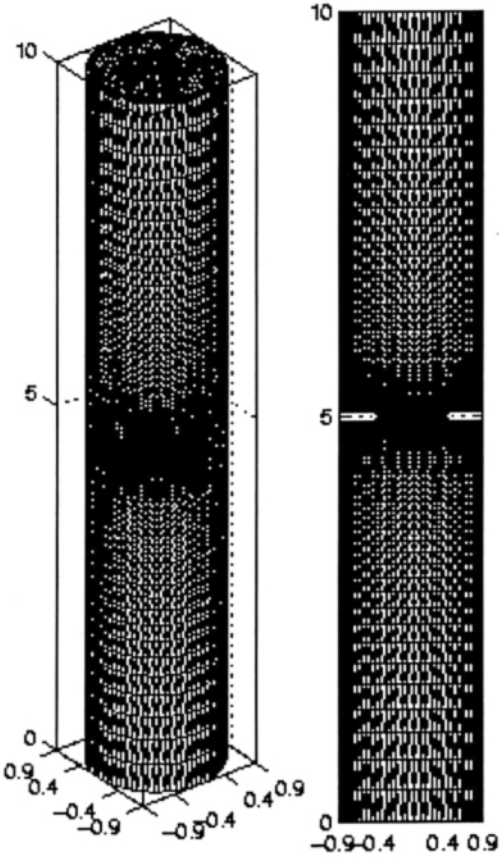

Figure 1. *Global fluid mesh*

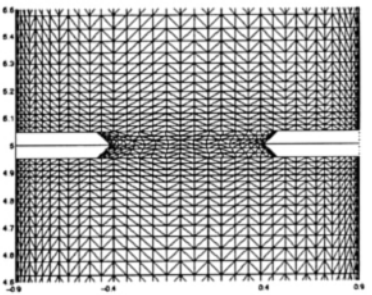

Figure 2. *Zoom on diaphgram.*

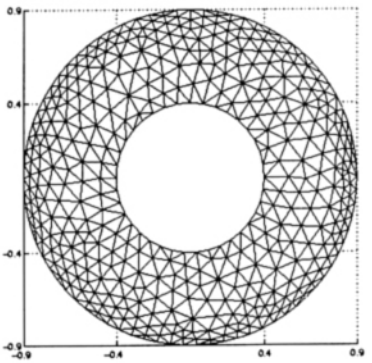

Figure 3. *Structure mesh*

around the jet are strong enough to induce some deviation of the jet. The flow is depicted in Fig. 4.

4. Structural modes

The structure is modelled through shell elements as shown in Fig. 3, the large circle is clamped, the small one being free. We depict in Fig. 5 the first correponding eigenmodes where mode 3 and mode 5 have been omitted since they are deduced by rotation from, respectively, modes 2 and 4. These modes are a good indication of possible coupled behaviors since the force induced by the fluid is rather uniform and normal to the shell.

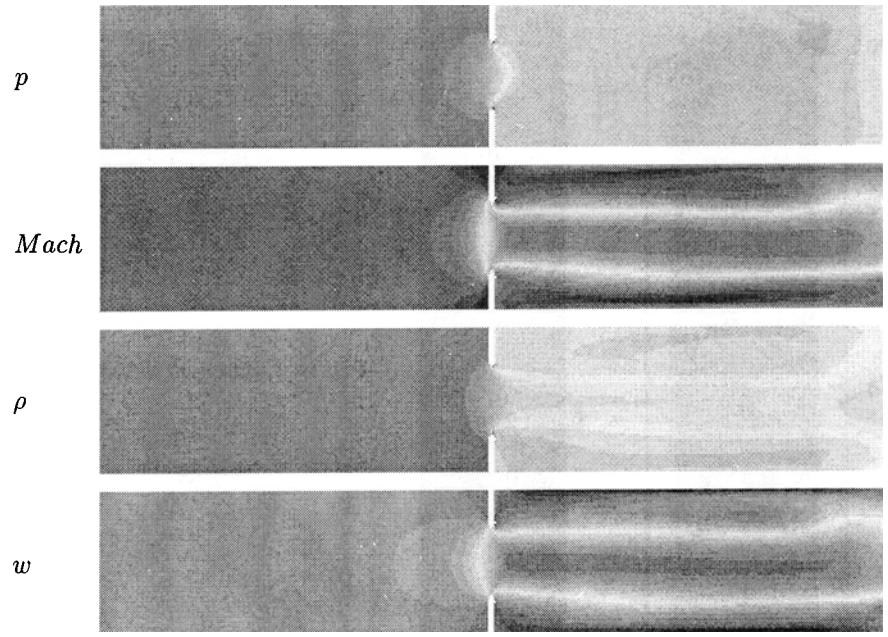

Figure 4. *Cut along a diametral plan of p, Mach, ρ and axial velocity w*

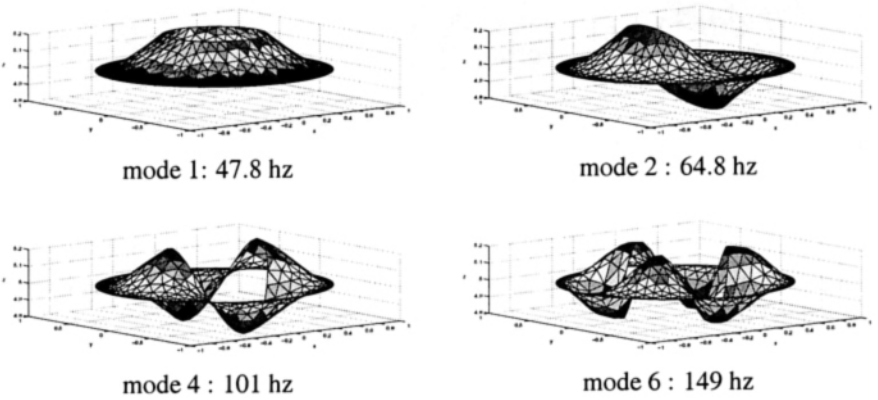

Figure 5. *Structure first eigenmodes*

5. Static effects

The influence of the flow on the structure is already important in the steady (non-pulsating) case, due to the large difference of pressure between upstream and downstream faces. In order to predict this static coupling, a purely numerical damping is

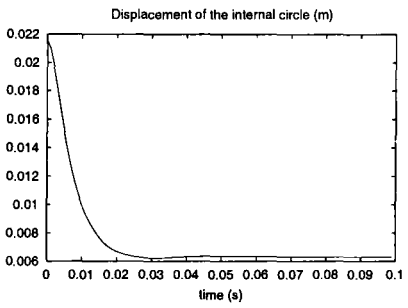

Figure 6. *Convergence to static*

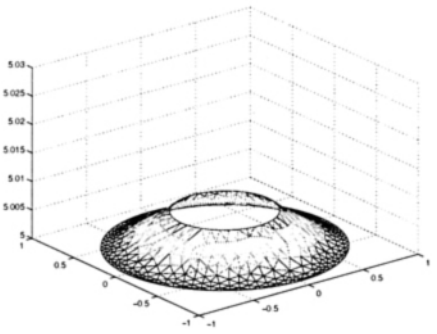

Figure 7. *Static shell shape*

introduced in the structural model (with a first-order time derivative). The structure initial condition is a deformed shape along its first mode and the time-step used is $\Delta t = 10^{-3}\ s$. Convergence is rather fast as shown in Fig. 6, and produces a structure shape, depicted in Fig. 7, that is different but close to the first eigenmode of the structure. The structure maximum displacement is at the inner circle and is equal to 6.2 mm, see Fig. 6.

6. Effects of inlet pulsations

The focus of the study is the understanding of possible scenarios in which the flow gives energy to the structure. The natural first context of investigation is to attempt to amplify the first eigenmode with a pulsating flow.

6.1. *Pulsation frequency set to the first structural eigenfrequency*

The test case conditions are a perturbation around those of the previous section. We sum up in short: inlet density $\rho_\infty = 1.3\ kg/m^3$, inlet pressure $p_\infty = 200000\ Pa$, inlet Mach number $M = 0.1$, therefore the reference inlet axial velocity is equal to $w_\infty = M_\infty \sqrt{\frac{\gamma p_\infty}{\rho_\infty}} = 46.4\ ms^{-1}$. The pulsation is imposed through the inlet axial velocity:

$$w_{\text{inlet}}(t) = w_\infty (1 + A \sin(2\pi f t))$$

where f represents the pulsating frequency set to the first structural eigenfrequency, i.e. $f = 47.78$ Hz and A is the fluctuation amplitude. We emphasize that the characteristic acoustic frequency estimated on the sound speed and half length of geometry is approximatively 47 Hz which is very close to the first structural eigenfrequency.

We will conduct two simulations for $A = 0.05$ and $A = 0.1$. The initial conditions for the flow and the structure are taken from the converged solution of the static computation described in section 5.

As expected, the structure is set into oscillation and the amplitude of motion is linearily amplified during the initial phase of the simulation (Fig. 8). After some time, *saturation* appears due to the non-linearity of the coupled system. An explanation may be that the force induced by the flow on the structure shows some decreasing (Fig. 9) when the structure takes its oscillating regime. Indeed, when the deformation of the membrane increases, the normal projection of the membrane surface decreases in conjunction with an increase of the radius of the internal circle creating a larger jet, both factors leading to a lower force applied on the structure.

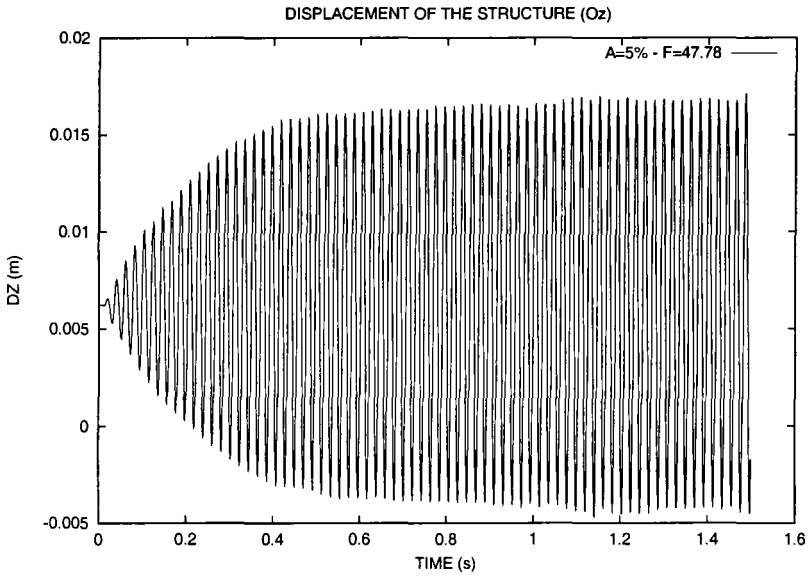

Figure 8. *Structure Displacement,* $A = 0.05$, $f = 47.78\ Hz$

The inlet velocity averaged over the inlet section is sketched in Fig. 10 and one can see that the amplitude of the velocity pulsation is time dependent. This is due to the use of "weak" boundary conditions which induces that the inlet velocity is influenced by the diaphragm motion and by informations coming from the upstream flow. One can also note that the aerodynamical force Cz presents some irregularities which, according to our knowledge, are produced by the recirculations located downstream of the diaphragm.

We have conducted the same simulation for a larger amplitude of fluctuation $A = 0.1$ and we have obtained very similar results. At saturation, one can see that there is a linear response between the measured amplitude of fluctuation of the mean inlet velocity $\Delta\overline{w}$ and the structure displacement amplitude Δz as shown in Table 1.

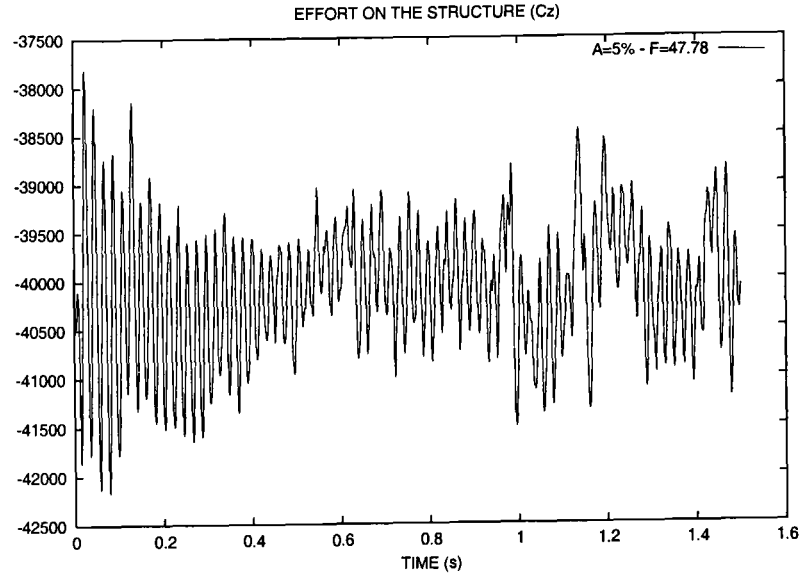

Figure 9. *Aerodynamical force Cz,* $A = 0.05$, $f = 47.78\ Hz$

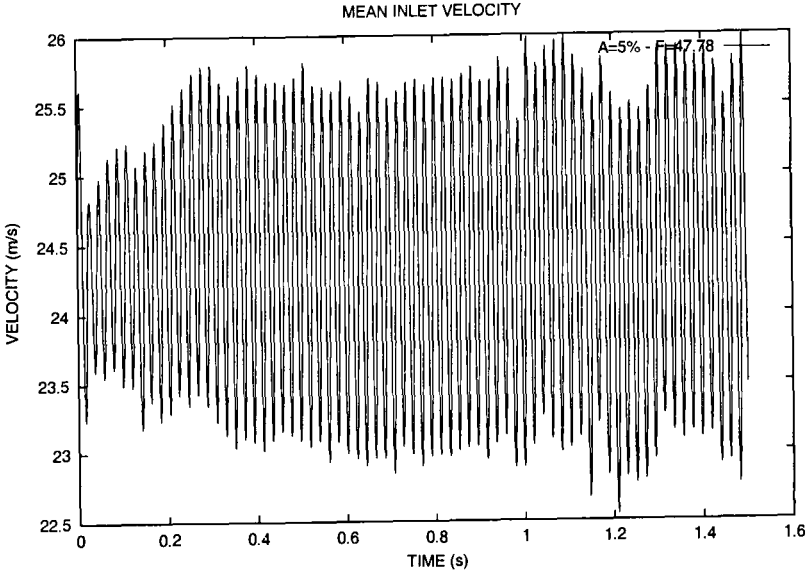

Figure 10. *Mean inlet velocity* $\overline{w}$, $A = 0.05$, $f = 47.78\ Hz$

6.2. *Influence of frequency*

In this section, we try to investigate the response of the coupled system to a pulsation sligthly different from the first eigenmode. The same inlet and initial conditions

A	$\Delta\overline{w}$	Δz	$\Delta\overline{w}$ / Δz
0.05	1.36 m/s	10.3 mm	0.1320
0.1	2.80 m/s	21.4 mm	0.1308

Table 1. *Influence of amplitude; mean inlet velocity and displacement*

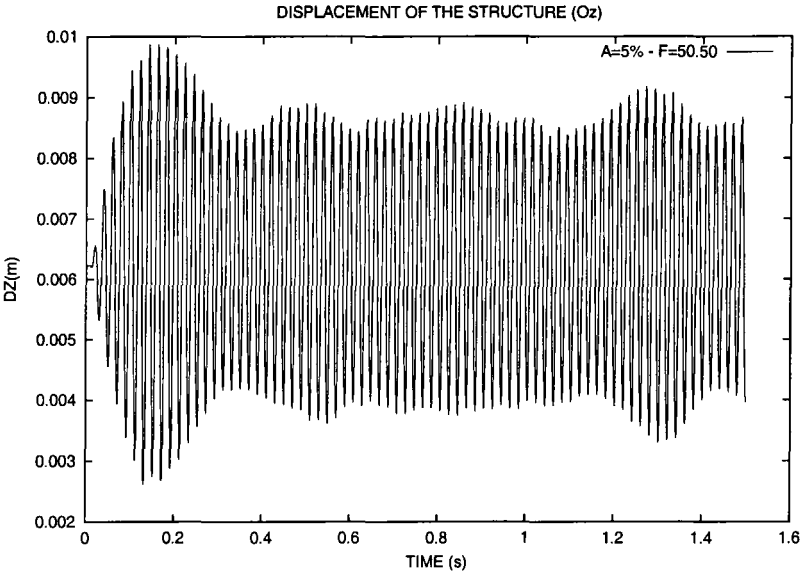

Figure 11. *Structure displacement, $A = 0.05$, $f = 50.5$ Hz*

are used with two pulsation frequencies of 50.5 Hz and 53 Hz and an amplitude of inlet velocity fluctuation of $A = 0.05$.

As expected, the amplitude of the diaphragm motion is lower than in the previous case, as seen in Fig. 11 and 12 and in Table 2. Both frequencies, the first eigenmode of the shell and the pulsating input are present in the transient of the simulations and one can see the low frequency corresponding to the frequency difference
(for $f = 50.5$ Hz, $T = 1/(47.8 - 50.5) = 0.37$ s;
and for $f = 53$ Hz, $T = 1/(47.8 - 53) = 0.19$ s). After this transient phase, the remaining frequency of the diaphragm motion is that of the inlet pulsation, the amplitude of motion remains quite constant showing that the first eigenmode has by then completely disappeared.

The figures 13 and 14 show that the pressure integral on the diaphragm is rather constant in time. One can point out that the aerodynamic force has the same mean level for the three frequencies ($\overline{C}_z = 4000$ N) but a much higher value of fluctuation amplitude is observed when the excitation frequency is not equal to the structure frequency, see Table 2.

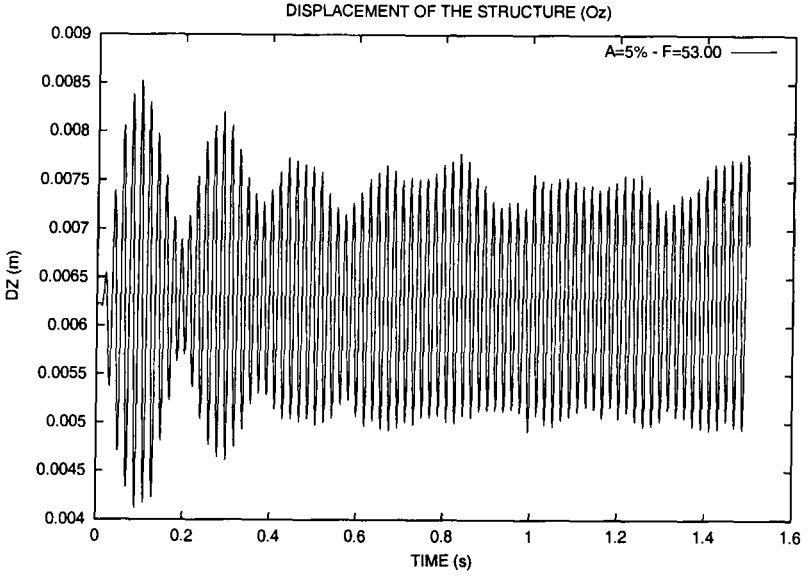

Figure 12. *Structure displacement,* $A = 0.05$, $f = 53\ Hz$

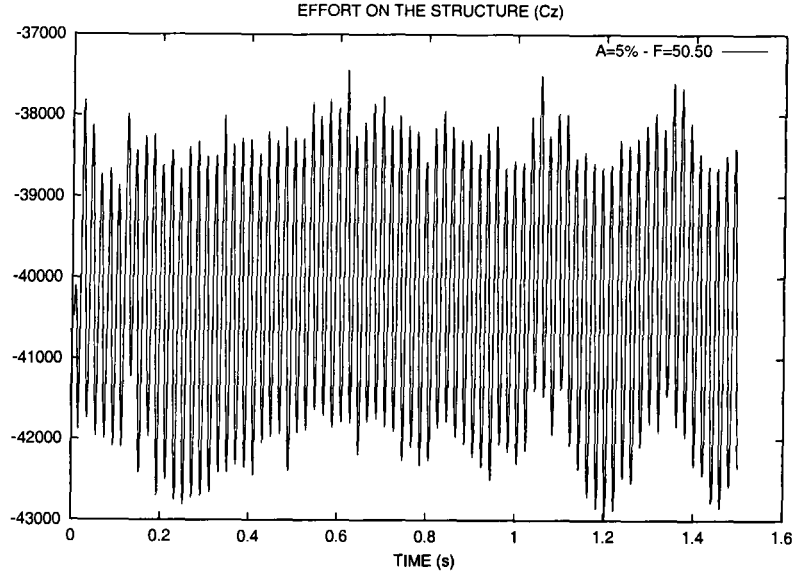

Figure 13. *Aerodynamical force Cz,* $A = 0.05$, $f = 50.5\ Hz$

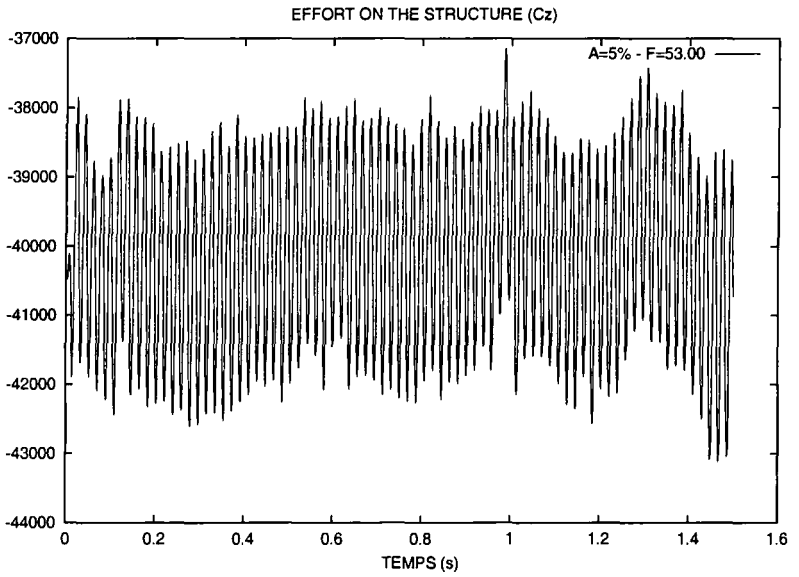

Figure 14. *Aerodynamical force Cz, $A = 0.05$, $f = 53$ Hz*

	$f = 47,78$ Hz	$f = 50.5$ Hz	$f = 53$ Hz
Displacement Δz	10.3 mm	2.4 mm	1.2 mm
Force ΔC_z	535 N	1940 N	1840 N

Table 2. *Influence of frequency; amplitude of displacement and force*

7. Conclusion

The 3D interaction of a pulsating flow and a diaphragm has been investigated. For this purpose, we have applied a sophisticated tool, involving complex CFD. The AERO software involves a Reynolds-Averaged Turbulence modelling that we shall also apply in the future. It also involves an accurate coupling method, with several features focusing on conservation of some trivial solutions and of energy through the interface. The global accuracy is of second-order, in time and space.

We do not have experiments to compare the numerical simulations with, but these numerical results will be used for a code to code comparison with the SNPE tool [MON 99], designed for predicting SRM thrust oscillation.

Looking a little more in details at the results, they confirm that axisymmetry is a rather robust property of the studied system, since no fully 3D deformation of the shell has been observed, even though the flow recirculation is nontrivially 3D. The axisymmetrical mode, conversely, is easily and fastly amplified by the pulsating flow.

Actually, a more decisive computation should involve the complete booster cavity, in which vortex shedding is naturally produced by the aeroacoustic effect. The coupling with structure might be one order of magnitude more complex. Such an application is one of the challenge of the SNPE code.

Acknowledgements

The authors acknowledge the support and the technical informations by CNES (Centre National d'Etudes Spatiales, France). Computations on ORIGIN 2000 were made possible thanks to Centre Charles Hermite at Nancy.

8. References

[SCH 99] SCHALL E., LARDAT R., DERVIEUX A., KOOBUS B., FARHAT C., " Investigation of the Aeroelastic Coupling between a Nozzle and a Supersonic Jet", *this issue.*

[LAR 00] LARDAT R., KOOBUS B., SCHALL E., DERVIEUX A., AND FAHRAT C., "Analysis of a Possible Coupling in a Thrust Inverter", *this issue.*

[CAR 99] CARPENTIER R.,"Le schéma $\beta-\gamma$ en axisymétrique", *INRIA research report* 3676, 1999.

[CAR 98] CARPENTIER R., HULIN A., "Numerical Unstable Modes in Unsteady Simulations of Natural Vortex Shedding" *Pressure Vessels and Piping Conference*, ASME/JSME, San Diego, July 26-30, 1998

[MON 99] MOMBELLI C., GUICHARD A., GODFROY F., GUERY J.-F., "Parallel Computation of Vortex-Shedding in Solid Rocket Motors", *35th AIAA/ASME/SAE/ASEE Joint Propulsion Conference*, Los Angeles, 20-24 June 1999.

[LEB 99] LEBRETON P., GUERY J.-F., PREVOST M., VUILLOT F., "Recent Advances in the Prediction of SRM Thrust Oscillations", *First European Conference on Launcher Technology*, Toulouse, 14-16 December 1999.

[GUI 98] GUILLARD H., VIOZAT C., "On the Behaviour of Upwind Schemes in the Low Mach Number Limit, *Comput. Fluids* 28, 1998, pp. 63-86

[FAR 95] FARHAT C., "High Performance Simulation of Coupled Non-Linear Transient Aeroelastic Problems", *AGARD Report* R-807, Special Course on Parallel Computing in CFD (l'Aérodynamique numérique et le calcul en parallèle, North Atlantic Treaty Organization (NATO), October 1995.

[FAR 98] FARHAT C., LESOINNE M. AND LE TALLEC P., "Load and Motion Transfer Algorithms for Fluid/Structure Interaction Problems with Non-Matching Discrete Interfaces: Momentum and Energy Conservation, Optimal Discretization and Application to Aeroelasticity", *Comp. Meth. in Applied Mech. and Eng.*, Vol. 157, pp. 95-114, 1998.